Cellular Microbiology (2012) **14**(6), 852–868
doi:10.1111/j.1462-5822.2012.01761.x
First published online 21 February 2012

Domain organization of *Legionella* effector SetA

Thomas Jank,[1] Kira E. Böhmer,[1] Tina Tzivelekidis,[1] Carsten Schwan,[1] Yury Belyi[2] and Klaus Aktories[1]*
[1]*Institut für Experimentelle und Klinische Pharmakologie und Toxikologie, Albert-Ludwigs-Universität Freiburg, Albertstr. 25, Freiburg D-79104, Germany.*
[2]*Gamaleya Research Institute, Ulitsa Gamalei 18, Moscow 123098, Russia.*

Summary

Legionella pneumophila **is a human pathogen causing severe pneumonia called Legionnaires' disease. Multiple *Legionella* effectors are type IV-secreted into the host cell to establish a specific vesicular compartment for pathogen replication. Recently, it has been reported that the *Legionella* effector SetA shares sequence similarity with glycosyltransferases and interferes with vesicular trafficking of host cells. Here we show that SetA possesses glycohydrolase and mono-*O*-glucosyltransferase activity by using UDP-glucose as a donor substrate. Whereas the catalytic activity is located at the N terminus of SetA, the C terminus (amino acids 401–644) is essential for guidance of SetA to vesicular compartments of host cells. EGFP-SetA expressed in HeLa cells localizes to early endosomes by interacting with phosphatidylinositol 3-phosphate. EGFP-SetA, transiently expressed in RAW 264.7 macrophages, associates with early phagosomes after infection with *Escherichia coli* and *L. pneumophila*. Only the combined expression of the C- and N-terminal domains induces growth defects in yeast similar to full-length SetA. The data indicate that SetA is a multidomain protein with an N-terminal glucosyltransferase domain and a C-terminal phosphatidylinositol 3-phosphate-binding domain, which guides the *Legionella* effector to the surface of the *Legionella*-containing vacuole. Both, the localization and the glucosyltransferase domains of SetA are crucial for cellular functions.**

Received 25 November, 2011; revised 13 January, 2012; accepted 17 January, 2012. *For correspondence. E-mail klaus.aktories@pharmakol.uni-freiburg.de; Tel. (+49) 761 203 5301; Fax (+49) 761 203 5311.

Introduction

Legionella pneumophila is a human pathogen causing Legionnaires' disease, a severe and often lethal pneumonia. The bacteria are taken up by alveolar macrophages where they replicate inside a specialized compartment, the *Legionella*-containing vacuole (LCV). LCV escapes lysosomal degradation and its establishment is accompanied by gross changes in cellular vesicle traffic. LCV formation involves the recruitment of various cellular organelles, including ribosomes, ER, Golgi and mitochondria, to its cytosolic membrane surface. To this end, *Legionella* produces hundreds of effector proteins, which are secreted by a type IV secretion system into the host cell cytosol. Only a few of these effector proteins are described in greater detail (Ninio and Roy, 2007; Ensminger and Isberg, 2009; Isberg *et al*., 2009; Hubber and Roy, 2010; Belyi *et al*., 2011).

Various *Legionella* effector proteins target small GTP-binding proteins, which regulate vesicular trafficking. For example, RalF activates the mammalian Arf1 protein, which controls vesicle formation at the Golgi (Nagai *et al*., 2002). Also Rab1, which controls vesicle trafficking in eukaryotic cells, is targeted by several *Legionella* effectors, including DrrA/SidM, LidA, LepB, SidD and AnkX (Machner and Isberg, 2006; Murata *et al*., 2006; Mukherjee *et al*., 2011; Neunuebel *et al*., 2011; Schoebel *et al*., 2011; Tan and Luo, 2011). Recently, versatile molecular mechanisms of these effectors to activate or inactivate GTP-binding proteins were unravelled, including the guanine nucleotide exchange factors (GEFs) RalF and SidM/DrrA (Nagai *et al*., 2002; Machner and Isberg, 2006), the Rab1-GTPase activating protein (GAP) LepB (Ingmundson *et al*., 2007), the Rab1 adenylyltransferase DrrA/SidM (Muller *et al*., 2010), the Rab1-supereffector LidA (Schoebel *et al*., 2011), the Rab1/Rab35 phosphocholine transferase AnkX (Mukherjee *et al*., 2011), the Rab1 de-AMPylation effector SidD (Neunuebel *et al*., 2011; Tan and Luo, 2011) and the Rab1 dephosphorylcholinase Lem3 (Tan *et al*., 2011).

Several other effector proteins were identified to target distinct steps in vesicular trafficking in yeast but the precise molecular mechanisms and their functions in mammalian cells are not known (de Felipe *et al*., 2005; Shohdy *et al*., 2005; Heidtman *et al*., 2009). Among these, *Legionella* effector Lpg1978 was identified and named SetA (subversion of eukaryotic traffic A) due to its role in subverting vesicular transport in yeast (Heidtman *et al*.,

2009). SetA is a 73 kDa protein and present in all sequenced pathogenic *L. pneumophila* strains. The group of Ralph Isberg (Heidtman *et al*., 2009) reported on the significant sequence similarity of SetA with glycosyltransferases, especially with enzymes of the family of clostridial glucosylating toxins like *Clostridium difficile* toxins A and B, which target small GTP-binding proteins of the eukaryotic Rho family (Just *et al*., 1995a; Aktories and Barbieri, 2005). Moreover, the N-terminal part of SetA possesses sequence similarity with the *Legionella* effector glucosyltransferases Lgt1, 2 and 3 (Belyi *et al*., 2008), which glucosylate eukaryotic elongation factor 1A thereby inhibiting protein synthesis (Belyi *et al*., 2006).

Here, we studied the structure-function relationship of SetA and its localization in target cells. We show by biochemical approaches that the N-terminal part possesses glucosyltransferase and glucohydrolase activity. In the cell, the C-terminal part guides SetA to early endosomes and exhibits colocalization mainly with Rab5. We report that vesicular interaction is regulated by binding of the C-terminal part of SetA to phosphatidylinositol 3-phosphate [PtdIns(3)P]. Both domains, the N-terminal glucosyltransferase domain and the C-terminal localization domain are necessary for the biological effect of SetA in eukaryotic cells.

Results

SetA is toxic to yeast and mammalian cells

To study the biological role of SetA in eukaryotic cell functions, we utilized *Saccharomyces cerevisiae* and expressed the *Legionella* effector with a galactose-inducible promoter. Expression of SetA caused a strong growth defect in yeast cells when cultivated on galactose-containing medium (Fig. 1A). These data corroborated recent findings by Isberg and co-workers (Heidtman *et al*., 2009). Scanning electron microscopy revealed that also yeast cell morphology changed upon induction with galactose, suggesting an alteration of fundamental cellular processes by SetA (Fig. 1B). To analyse the effect of SetA in mammalian cells, recombinantly expressed SetA and the inactive mutant SetA NXN ($N^{134}XN^{136}$), which possesses a double amino acid exchange in the conserved DXD motif of glycosyltransferases (Busch *et al*., 1998; Heidtman *et al*., 2009), was microinjected into embryonic bovine lung (EBL) cells and cellular changes were monitored by live cell imaging for 8 h (Fig. 1C and D, Movies S1 and S2). After 6–8 h, cells retracted. This effect was only seen with wild-type SetA (Fig. 1C). The inactive mutant SetA NXN did not induce any cellular alterations (Fig. 1D). Thus, these data suggest that the proposed glucosyltransferase activity of SetA is responsible for the phenotypic alterations observed not only with yeast but also with mammalian cells.

UDP-glucose is the donor substrate of SetA

Most known glucosyltransferases use nucleotide sugars, usually UDP-sugars, as activated sugar donor substrates in glycosylation reactions. Moreover, many glycosyltransferases possess glycohydrolase activity and cleave donor sugar substrates in the absence of their acceptor substrate. This is especially true for the SetA-related glucosyltransferases like the clostridial glucosylating toxins (Busch *et al*., 1998). To identify the donor substrate of SetA, we used various radiolabelled UDP-[^{14}C]sugars and compared the hydrolase activity of SetA with these substrates using thin layer chromatography (Fig. 2A). The glucosyltransferase domain of *C. difficile* toxin B was used as reference. UDP-[^{14}C]glucose was cleaved most efficiently with a k_{cat} of 225.6 $\pm$ 20.3 h^{-1} comparable to toxin B. Additionally, several non-labelled nucleotide sugars were applied in molar excess to compete with UDP-[^{14}C]glucose. Solely, UDP-glucose and to a certain degree UDP alone were able to compete with radiolabelled UDP-[^{14}C]glucose revealing UDP-glucose as the possible donor substrate of SetA (Fig. 2B).

Catalytic activity is restricted to the N-terminal 300 amino acids of SetA

We expressed several truncations of SetA (Fig. 3A) in *Escherichia coli* as His-tagged proteins, removed the tag by tobacco etch virus protease cleavage and analysed the constructs for glucohydrolase activity (Fig. 3B). Glucohydrolase activity was detected with fragments harbouring the N-terminal 300 amino acids, but not with the C-terminal fragment $SetA^{301–644}$. For maximal hydrolase activity the N-terminal 400 amino acids were crucial. Furthermore, we observed auto-glucosylation of SetA, when UDP-[^{14}C]glucose was used as a donor substrate. Figure 3C shows that the auto-glucosylation activity was also determined with the N-terminal 300 amino acids fragment of SetA, assuming that a functional glucosyltransferase domain is located within the N-terminal half of the protein. So far, however, we did not identify the acceptor substrate of SetA. Therefore, we tested several proteins with distinct acidic and basic characteristics as *in vitro* substrates for glucosylation by SetA. We observed that histone proteins from calf thymus were readily glucosylated (Fig. 3D). Glucosylation of histones seemed to be specific, because toxin B, the related glucosyltransferase from *C. difficile*, did not show any histone glucosylation. Mass spectrometric analysis of histones, modified by SetA, revealed a mono-*O*-glucosylation of histones H4 and H3.1 at threonine and serine residues (Thr-81 and Thr-83 in H4; Ser-58 and Thr-81 in H3.1, data not shown). Using histones as model substrates for SetA we observed that SetA constructs, harbouring the first 300 amino acids possessed glucosyl-

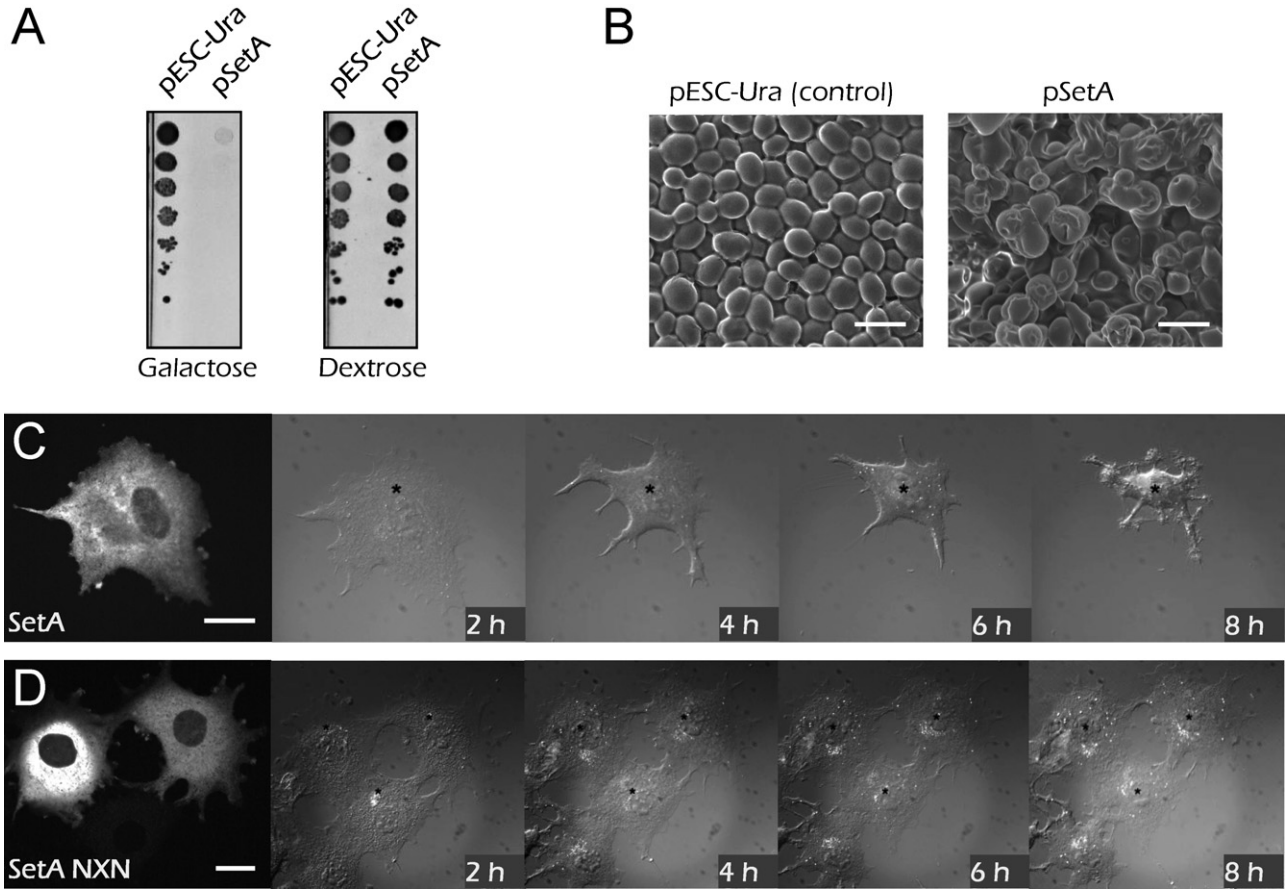

Fig. 1. Toxicity of SetA to eukaryotic cells.
A. Growth of yeast cells expressing SetA from a galactose-inducible promoter (pSetA) on dextrose medium or on galactose medium. Yeast strains harbouring an empty vector (pESC-Ura) were used as control. Fivefold serially diluted yeast cultures grown in glucose medium were spotted followed by incubation at 37°C for 2 days.
B. Expression of SetA alters yeast cell morphology. Scanning electron microscopic pictures of *S. cerevisiae* expressing SetA (pSetA) or vector alone (pESC-Ura control). Yeasts were subjected to microscopy after growth in SD + Gal medium for 4 days. Scale bar, 5 μm.
C and D. Toxicity of SetA to mammalian cells. Recombinant SetA (5 μg μl^{-1}) (C) or the catalytic inactive DXD mutant (SetA NXN, 5 μg μl^{-1}) (D) were microinjected into embryonic bovine lung (EBL) cells. Cells were photographed each minute for 8 h (see Movies S1 and S2). Selected images are depicted. Microinjected cells were distinguished by co-injection of Alexa488- and Alexa568-labelled antibodies [see immunofluorescent images in the first panel of (C) and (D)]. Injected cells are marked with an asterisk. Scale bar, 20 μm.

transferase activity comparable to the full-length protein (Fig. 3D). The C-terminal fragment ($SetA^{301–644}$) or the SetA NXN mutant exhibited no transferase activity.

The C-terminal domain of SetA (aa 401–644) binds to vesicles in mammalian cells

Recently, Isberg and co-workers reported that SetA localizes to vesicular structures when expressed in HeLa cells (Heidtman *et al*., 2009). We confirmed these data by the ectopical expression of various fluorescently tagged SetA constructs (EGFP, mCherry, DsRed). The rather late cytotoxic effect (Fig. 1C) allowed transient expression of EGFP-SetA and analysis of the localization by confocal microscopy and life cell imaging (Movie S3). Full-length SetA localized to the cytosolic leaflet of highly motile vesicular structures located in the cytoplasm of the cells. Furthermore, we identified the minimal region of SetA responsible for its subcellular localization to vesicles. Therefore, we constructed several truncation mutants (Fig. 4A) and expressed these as EGFP-fusion proteins in HeLa cells (Fig. 4B). Only C-terminal constructs, including amino acids 401–644, were localized to vesicular structures inside the cell. Thus, these findings suggest that the C-terminus (amino acids 401–644) harbours the localization domain, which guides SetA to vesicular structures inside the host cell.

SetA is recruited by early endosomes

To identify the type of vesicles which are targeted by SetA, we transiently transfected HeLa cells with EGFP-SetA

A

	k_{cat} [h^{-1}]	rel. k_{cat}
UDP-[^{14}C]glucose	225.6 ± 20.3	1
UDP-[^{14}C]galactose	7.8 ± 0.8	0.035
UDP-[^{14}C]GlcNAc	2.0 ± 0.2	0.0087
UDP-[^{14}C]glucose (Toxin B1-546)	274.5 ± 24.4	1.22

B

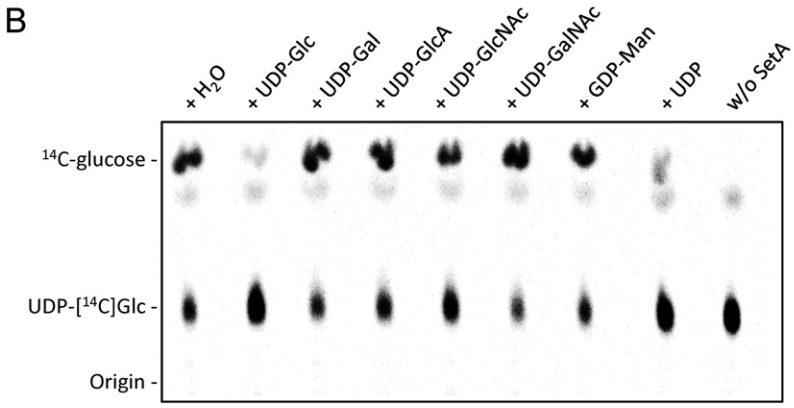

Fig. 2. UDP-glucose is the donor substrate of SetA.
A. Table of kinetic values for hydrolase activity of SetA. SetA (50 nM) was incubated with 10 μM of the indicated UDP-sugars for 30 min at 30°C. The initial velocities of the hydrolase reaction were determined by thin layer chromatography and autoradiography. The catalytic domain of *Clostridium difficile* toxin B (Toxin B1-546) was used as reference glucosyltransferase (data shown are the mean of at least three independent experiments ± SD).
B. Glucohydrolase activity of SetA was performed with SetA (200 nM) in the presence of 10 μM UDP-[^{14}C]glucose and without (lane 1) or with (lanes 2–9) 100 μM of each unlabelled compound: UDP-glucose (UDP-Glc), UDP-galactose (UDP-Gal), UDP-glucuronic acid (UDP-GlcA), UDP-*N*-acetylglucosamine (UDP-GlcNAc), UDP-*N*-acetyl-galactosamine (UDP-GalNAc), GDP-mannose and UDP. After incubation for 90 min at 30°C in a buffer, containing 50 mM Hepes pH 7.4, 2 mM $MgCl_2$ and 1 mM $MnCl_2$, 800 nl were applied to polyethyleneimine thin layer chromatography with 0.2 M LiCl as mobile phase. The separated radiolabelled reaction products were analysed by phosphorimaging and quantified with ImageQuant.

and analysed its colocalization with specific endosomal marker proteins (Fig. 5). Rab11 was used as a marker for recycling endosomes (Fig. 5A). Rab5 (Fig. 5B) and early endosomal antigen 1 (EEA1) (Fig. 5C) were used as markers for early endosomes. Moreover, Alexa568-labelled transferrin was employed as an early endosomal marker, which exhibited association with Rab5-containing vesicles 10 min after addition to the cell culture medium (Fig. 5D). Rab7 was used as a late endosomal marker (Fig. 5E) and LAMP1 as a marker for lysosomes (Fig. 5F). Rab9 was used to distinguish vesicles shuttling between the trans-Golgi network and late endosomes (Fig. 5G). We determined the percentage of colocalization of SetA (green) with the indicated markers (red) and *vice versa*. The degree of colocalization was in the following order: Rab5 > EEA1 > transferrin > Rab7 > LAMP1 > Rab9 > Rab11. Rab5 colocalization with SetA was additionally analysed by life cell imaging (Movie S4). All these data suggest that SetA is attracted specifically by early endosomes.

SetA binds highly specific to phosphatidylinositol 3-phosphate

Next, we asked which component of the early endosomal outer leaflet is responsible for the highly specific recruitment of SetA. We suggested that phosphoinositides are possible candidates for an interaction with SetA, because they have been shown to be tightly regulated by phosphorylation and dephosphorylation during endocytic transportation and serve as binding platforms for distinct eukaryotic as well as prokaryotic protein domains (De Camilli *et al*., 1996; Cho and Stahelin, 2005; Di Paolo and De Camilli, 2006; Hurley, 2006; Lemmon, 2008; Weber *et al*., 2009a). For example it was shown that phosphatidylinositol 3-phosphate [PtdIns(3)P] is specifically enriched in early endosomal membranes and forms an interacting platform for various PX- or FYVE-domain containing proteins (Gillooly *et al*., 2003). Therefore, we used the p40phox PX domain of NADPH oxidase as a PtdIns(3)P-binding domain (Bravo *et al*., 2001; Ellson *et al*., 2001; Sato *et al*., 2001). After cotransfection of HeLa cells with EGFP-SetA and DsRed-p40phox, we analysed the localization of both constructs (Fig. 6A). Strikingly, EGFP-SetA colocalized with DsRed-p40phox by 74.5 ± 6.8% and DsRed-p40phox with EGFP-SetA by 81.7 ± 14.9%. These results suggest a specific interaction of SetA with PtdIns(3)P.

Next, we used protein-lipid overlay assays to prove these findings (Fig. 6B). Nitrocellulose membranes, prespotted with different lipids, were overlayed with the GST-fused proteins GST-SetA, the N-terminal glucosyltransferase domain GST-SetA^{300}, the C-terminal localization domain GST-SetA$^{401–644}$ and as a control GST-SidC, a variant effector of *L. pneumophila*, which specifically binds PtdIns(4)P (Weber *et al*., 2006). According to subcellular localization experiments (Fig. 4), only full-length SetA and the C-terminal domain bound significantly to

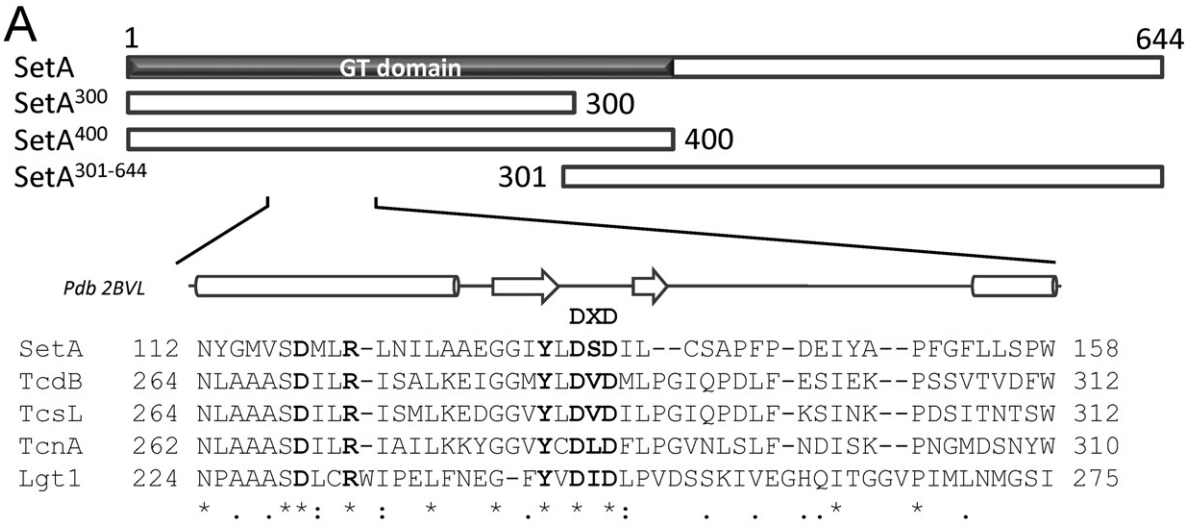
A
1
644
SetA
GT domain
SetA300
300
SetA400
400
SetA301-644
301
Pdb 2BVL
DXD
SetA 112 NYGMVSDMLR-LNILAAEGGIYLDSDIL--CSAPFP-DEIYA--PFGFLLSPW 158
TcdB 264 NLAAASDILR-ISALKEIGGMYLDVDMLPGIQPDLF-ESIEK--PSSVTVDFW 312
TcsL 264 NLAAASDILR-ISMLKEDGGVYLDVDILPGIQPDLF-KSINK--PDSITNTSW 312
TcnA 262 NLAAASDILR-IAILKKYGGVYCDLDFLPGVNLSLF-NDISK--PNGMDSNYW 310
Lgt1 224 NPAAASDLCRWIPELFNEG-FYVDIDLPVDSSKIVEGHQITGGVPIMLNMGSI 275
* . .**: * : * * .* * *: . . ..* * .

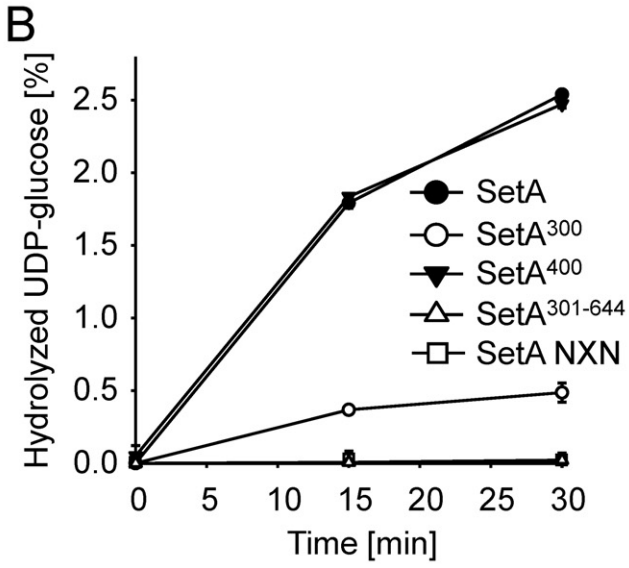
B
Hydrolyzed UDP-glucose [%]
2.5
2.0
1.5
1.0
0.5
0.0
0
5
10
15
20
25
30
Time [min]
SetA
SetA300
SetA400
SetA301-644
SetA NXN

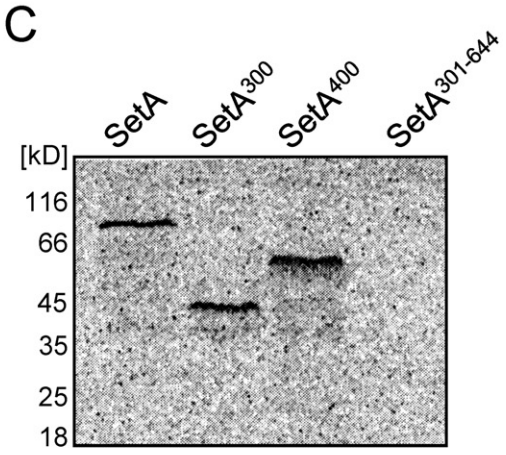
C
SetA
SetA300
SetA400
SetA301-644
[kD]
116
66
45
35
25
18

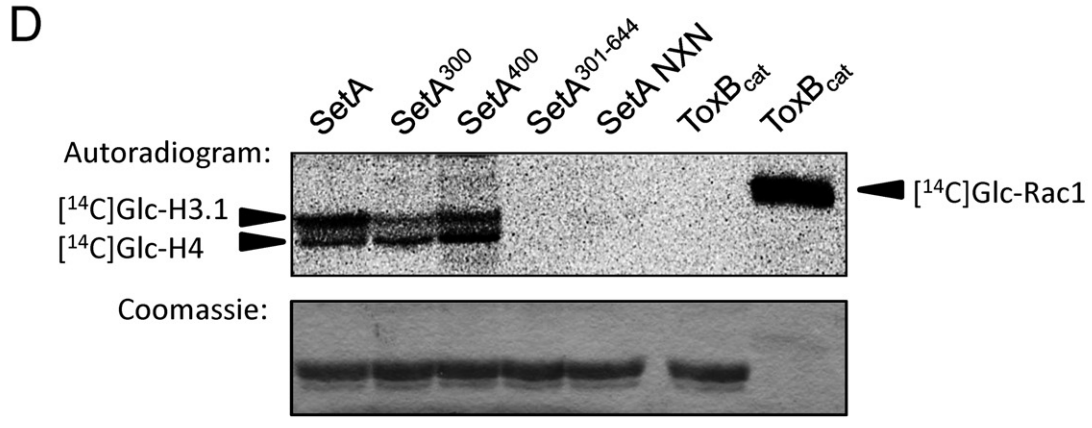
D
SetA
SetA300
SetA400
SetA301-644
SetA NXN
ToxBcat
ToxBcat
Autoradiogram:
[14C]Glc-H3.1
[14C]Glc-H4
[14C]Glc-Rac1
Coomassie:

Fig. 3. Enzymatic activity of SetA is restricted to the N-terminus.
A. Schematic representation of the SetA truncation constructs used for analysing enzymatic activity. The alignment represent sequence similarities surrounding the DXD motif between SetA (Lpg1978), the clostridial glucosylating toxins [*Clostridium difficile* toxin B (TcdB), *C. sordellii* lethal toxin (TcsL), *C. novyi* α-toxin (TcnA)] and *Legionella* glucosyltransferase 1 (Lgt1). The secondary structural elements refer to the crystal structure of *C. difficile* toxin B (pdb 2BVL). Bold amino acids are conserved and were shown to have crucial functions in glycosylation reaction of the clostridial glucosylating toxins (Busch *et al*., 1998; Jank *et al*., 2007). Conserved amino acids are marked with an asterisk; similar amino acids are marked with dots.
B. Time-course of glucohydrolase activity of SetA-truncations. Enzymatic hydrolysis of UDP-[^{14}C]glucose (10 μM) was performed with SetA, SetA^{300}, SetA^{400}, SetA$^{301–644}$ and SetA NXN (each 70 nM) at 30°C for 60 min. At the indicated time points the products were separated by thin layer chromatography and analysed autoradiographically. The amount of UDP-glucose hydrolysis was quantified by ImageQuant. The mean of three experiments ± SD is shown.
C. Autoglucosylation of SetA-truncations. SetA, SetA^{300}, SetA^{400} and SetA$^{301–644}$ (each 1 μM) were incubated with 50 μM UDP-[^{14}C]glucose for 60 min at 30°C in a buffer, containing 10 mM Hepes pH 7.4, 2 mM $MgCl_2$ and 1 mM $MnCl_2$. Radiolabelled proteins were separated by SDS-PAGE and visualized using autoradiography.
D. Glucosylation of the *in vitro* substrates histone H4 (11.4 kD) and H3.1 (15.4 kD). Histone preparation from calf thymus (10 μg) was incubated with the constructs SetA, SetA^{300}, SetA^{400}, SetA$^{301–644}$ and SetA NXN (each 1 μM) in the presence of UDP-[^{14}C]glucose (50 μM) for 60 min at 30°C. As control the glucosyltransferase domain of *C. difficile* toxin B (100 nM) was used with histones and Rac1 (0.5 μg) as its natural substrate. Radiolabelled histones were analysed by SDS-PAGE and autoradiography.

PtdIns(3)P (Fig. 6B), but not the N-terminal glucosyltransferase domain. To corroborate these data, we used a PIP array with serially diluted lipids ranging from 1.56 to 100 pmol spotted onto nitrocellulose membranes and probed with the GST-fusion proteins GST-SetA, GST-SetA$^{401–644}$ and GST-p40phox PX domain [PtdIns(3)P-binding control] (Fig. 6C). The specificity of the interaction of SetA with PtdIns(3)P was comparable to the binding of the p40phox PX domain. To obtain conditions resembling vesicular compartments, we produced liposomes containing PtdIns(3)P or PtdIns(4)P. In addition, we prepared liposomes without phosphoinositides as control, and tested the binding to GST-SetA or GST-SidC. After extensive washing steps, the liposomes were subjected to Western blotting and probed with anti-GST antibody (Fig. 6D). GST-SetA was specifically bound to PtdIns(3)P-containing liposomes, whereas GST-SidC that is known to interact with PtdIns(4)P (Weber *et al*., 2006; Ragaz *et al*., 2008), was predominantly bound to PtdIns(4)P-containing liposomes. These results confirmed the binding specificity of SetA to PtdIns(3)P obtained with the overlay assay.

SetA interacts with phosphatidylinositol 3-phosphate with high affinity

To study the affinity of SetA to PtdIns(3)P in more detail, we used surface plasmon resonance spectroscopy. To this end, biotin-labelled PtdIns(3)P (Fig. 7C) was coupled onto a streptavidin-coated sensor chip and the binding of SetA to the surface of the chip was analysed. The sensogram in Fig. 7A shows SetA-binding to the PtdIns(3)P derivative in a concentration dependent manner. Equilibrium binding analyses revealed a K_d value of 809 ± 51 nM (Fig. 7B), which is in the range of the affinity of the p40 phox PX domain (K_d = 431 ± 27 nM) (Fig. S1C). BSA and GST served as a control, giving no measurable resonance signal (data not shown and Fig. S1D). The glucosyltransferase domain of SetA did not influence the affinity to the phosphatidylinositide whereas the catalytic deficient NXN-mutant or the C-terminal fragment SetA$^{301–644}$ exhibited a similar K_d value of 1.01 ± 0.21 μM or 1.45 ± 0.28 μM, respectively (Fig. S1A and B).

SetA is recruited to the Legionella*-containing phagosome*

As we identified the C-terminal domain of SetA as a localization domain targeting SetA to PtdIns(3)P-containing compartments, we attempted to visualize the localization of SetA in the context of bacterial phagocytosis. We transfected RAW 264.7 macrophages with pmCherry-SetA or pEGFP-SetA and applied GFP-expressing *E. coli* or *L. pneumophila* serogroup 1 Philadelphia 1 for monitoring phagocytosis. As shown in Fig. 8, mCherry-SetA (red) and EGFP-SetA (green) localized to phagosomes, containing GFP-expressing *E. coli* (green; A) and immunostained *L. pneumophila* (red; B) respectively. We quantified the amount of bacteria-containing vesicles colocalizing with fluorescent labelled SetA and found that 91.9 ± 7.1% (±SD; n = 3) of *E. coli*-containing vesicles and 79.3 ± 14.5% (±SD; n = 3) of *Legionella*-containing vesicles were associated with fluorescent labelled SetA.

Full-length SetA is necessary for cellular effects

Our results showed that SetA can be distinguished into at least two distinct domains, the N-terminal glucosyltransferase domain and the C-terminal localization domain. Using yeast as a model system, we wanted to know which domain is crucial for cellular effects. As shown in Fig. 1A, expression of SetA in yeast caused a severe growth defect. We analysed full-length SetA, the NXN-mutant, the N-terminal parts SetA^{300} and SetA^{400} and the C-terminal domain SetA$^{301–644}$ and expressed the separate domains in yeast (Fig. 9). Only expression of full-length SetA induced

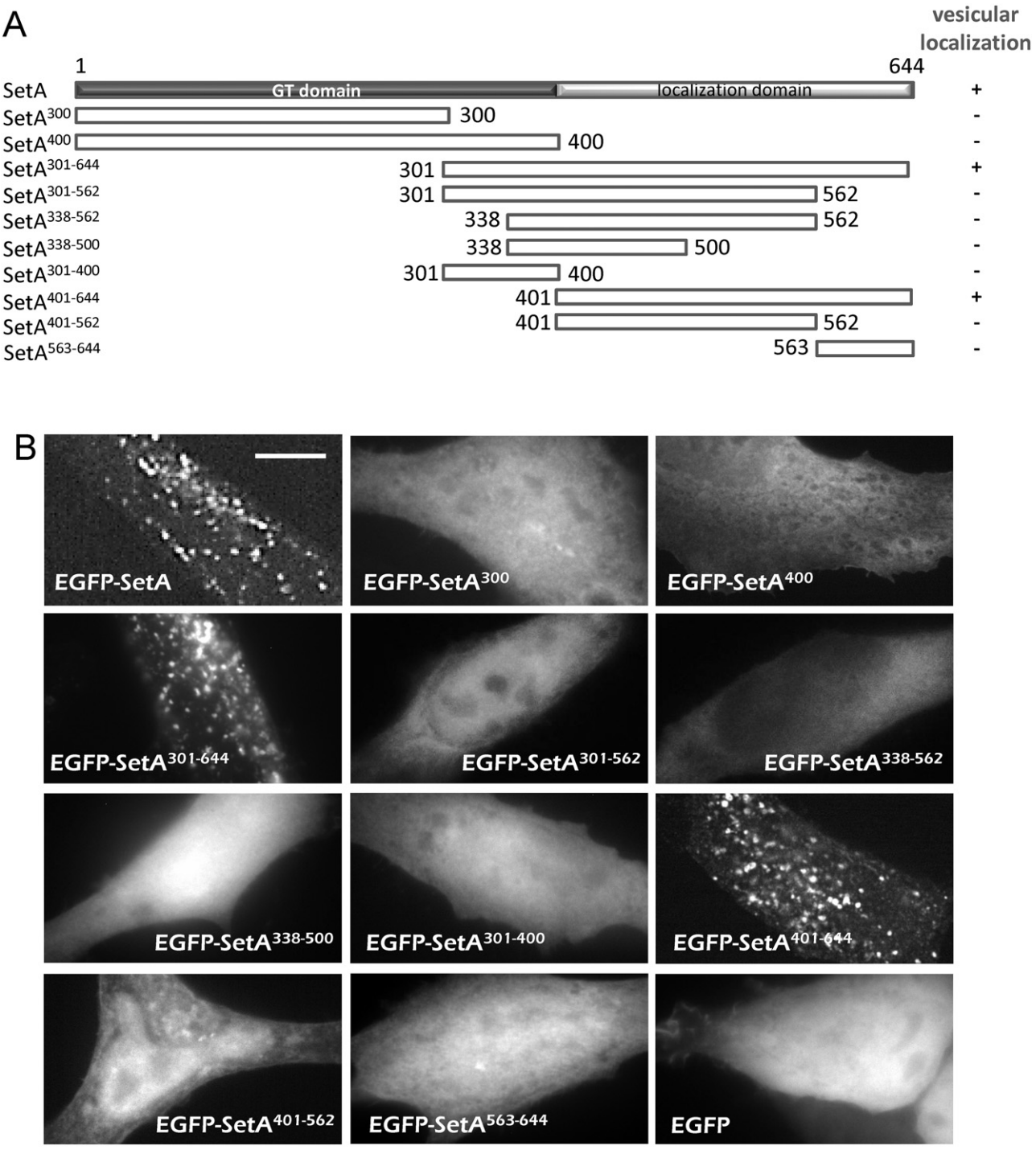

Fig. 4. C-terminus of SetA associates with vesicular structures of HeLa cells.
A. Schematic representation of the EGFP-truncation constructs used for ectopical expression and localization studies in HeLa cells. Right panel: SetA constructs localizing to vesicular compartments are marked with (+), localization throughout the cell is marked with (–).
B. HeLa cells were transiently transfected with the EGFP-SetA truncation constructs depicted in (A) and with EGFP as a control. After 6 h cells were fixed with 4% PFA and analysed microscopically. Representative fluorescent micrographs are shown. Scale bar, 10 μm.

a strong growth inhibition phenotype, whereas the separated C-terminal domain and the glucosyltransferase domain (SetA^{400}) caused only slight growth retardation. However, when we expressed the genes coding the active glucosyltransferase domain (SetA^{400}) and the C-terminal localization domain (SetA$^{301–644}$) delivered together on separate vectors (pESC-Ura and pESC-His correspondingly), a typical growth defective phenotype was revealed (Fig. 9). In summary, our data suggest that both domains, the glucosyltransferase domain and the localization domain of *Legionella* effector SetA are essential for the cellular effects on the eukaryotic host.

Discussion

Here we analysed the *Legionella pneumophila* effector protein SetA, which is secreted by a type IV secretion system into the host cell cytosol. A recent study by Isberg and co-workers suggested that SetA is involved in subversion of eukaryotic vesicle trafficking (Heidtman *et al*., 2009). Although the sequence similarity of SetA with glycosyltransferases has been described (Heidtman *et al*., 2009), no glycosyltransferase or glycohydrolase activities were shown. In the present study we dissected SetA into two distinct domains and characterized their function in more detail. We could show that the N-terminal domain (aa 1–400) possesses glycosyltransferase- and glycohydrolase activity, whereas the C-terminal part of SetA (aa 401–644) harbours a localization domain, which binds to a specific phosphoinositide [PtdIns(3)P] and thereby guides SetA to the cytosolic leaflet of the early phagosome of the host cell.

The N-terminal part of SetA exhibits significant sequence similarity with glycosyltransferases, especially with the clostridial glucosylating toxins like *C. difficile* toxins A and B, which modify Rho proteins by mono-*O*-glucosylation (Just *et al*., 1995a,b; Heidtman *et al*., 2009). Moreover, sequence similarity is found with *Legionella* effectors Lgt1-3, which cause glucosylation of eEF1A (Belyi *et al*., 2006). A typical structural feature of these glycosyltransferases is the DXD motif, which is involved in phosphate and divalent cation (e.g., manganese) coordination (Busch *et al*., 1998; Reinert *et al*., 2005). This DXD motif is also found in SetA (Heidtman *et al*., 2009). Up to date no glucosyltransferase activity of SetA has been reported. Most glucosyltransferases possess glycohydrolase activity in the absence of their sugar acceptor substrate. However, also no glycohydrolase activity of SetA was reported so far. Here we present evidence that SetA possesses glucohydrolase and glucosyltransferase activities. Glucohydrolase activity of SetA was most prominent with the substrate UDP-glucose. Moreover, unlabelled UDP-glucose but no other nucleotide sugars largely reduced hydrolysis of radiolabelled UDP-[^{14}C]glucose, indicating a preference for this activated sugar molecule. Although we were not able to identify the endogenous eukaryotic substrate of SetA *in vivo*, we show that the *Legionella* effector induces a glucosyltransferase reaction with *in vitro* protein substrates. In the presence of UDP-glucose, histones H3.1 and H4 were glucosylated by SetA. Mass spectrometric analysis revealed that threonine and serine residues were modified by mono-*O*-glucosylation. Histones are primarily located in the nucleus. Our experiments showed that HeLa cells expressing EGFP-SetA or N-terminal fragments of SetA were not located to the nucleus but were associated with cytosolic vesicles or distributed in the cytoplasm respectively (Fig. 4B). Therefore, it is unlikely that histones are the natural substrates for SetA. Beside histone glucosylation, we observed a strong auto-glucosylation of SetA in the presence of UDP-glucose. The activities (glucosylation and glucohydrolase activity) were completely abolished by changing the crucial DXD motif of SetA. Thus, all these data indicate that SetA is a glucosyltransferase, which possesses glycohydrolase activity and uses UDP-glucose as the sugar donor. Moreover, this activity could be restricted to the N-terminal 300 amino acids of the molecule.

The second part of the study focused on the function of the C-terminus of SetA and its role in intracellular localization. Isberg and co-workers analysed SetA colocalization with Rab7 and LAMP1 and postulated an interaction of SetA with late endosomal or lysosomal compartments (Heidtman *et al*., 2009). Our localization studies performed with various fluorescent SetA fusion proteins also support the view that SetA interacts with vesicles. However, we observed a predominant colocalization of SetA with Rab5 and early endosomal antigen 1 (EEA1), which are both markers for early endosomes. These data were supported by the findings that SetA interacted predominantly with vesicles, which had taken up Alexa568-labelled transferrin. Transferrin is the cargo of the transferrin receptor, which is internalized by clathrin-mediated endocytosis into early endosomes, where it releases the iron and recycles back to the plasma membrane (Mayle *et al*., 2011). Transient transfected SetA colocalizes with Alexa568-labelled transferrin but is not colocalizing with Rab11-containing recycling endosomes. Therefore, the data suggest that vesicles harbouring SetA belong to the early endocytic compartments and SetA does not reach late endosomal or lysosomal vesicles. Our results suggest that SetA interacts with early endosomes by a specific and high affine interaction with PtdIns(3)P, which is particularly enriched on early endosomes (Gillooly *et al*., 2003). We employed the p40phox subunit of NADPH oxidase as a marker for PtdIns(3)P colocalization. Moreover, the interaction of SetA with PtdIns(3)P was confirmed in overlay assays

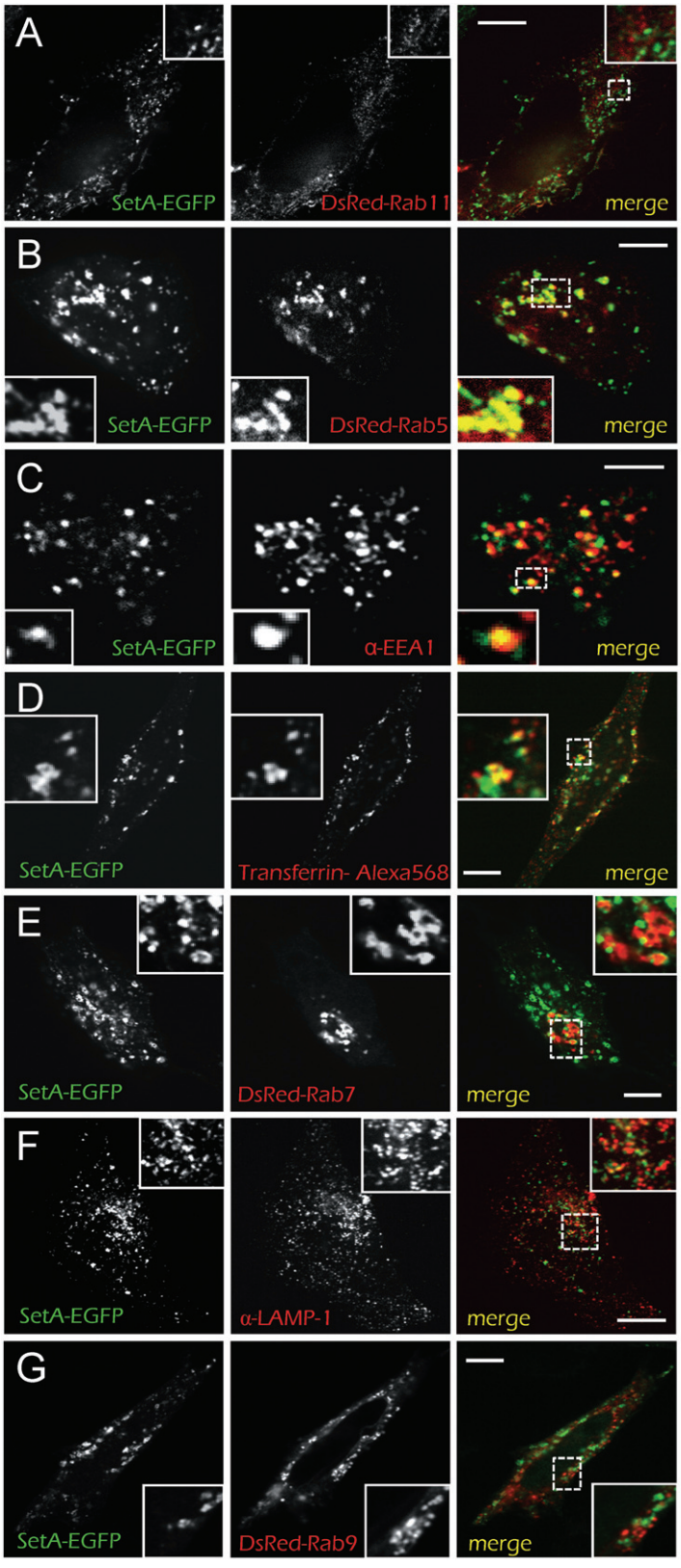

H **Colocalization [% of Total]**

SetA with Rab11	8.0 ± 7.1 %
Rab 11 with SetA	12.5 ± 7.8 %
SetA with Rab5	72.7 ± 10.1 %
Rab5 with SetA	68.8 ± 19.5 %
SetA with EEA1	65.8 ± 10.9 %
EEA1 with SetA	44.3 ± 8.8 %
SetA with Tf	58.3 ± 8.6 %
Tf with SetA	44.4 ± 10.1 %
SetA with Rab7	23.8 ± 9.2 %
Rab 7 with SetA	32.2 ± 14.2 %
SetA with LAMP1	19.8 ± 12.9 %
LAMP1 with SetA	15.4 ± 6.5 %
SetA with Rab9	11.6 ± 7.2 %
Rab9 with SetA	9.8 ± 7.7 %

Fig. 5. Colocalization of SetA with early endosomal markers. HeLa cells were transiently transfected with EGFP-SetA (left, green) and analysed for colocalization with specific marker proteins for endocytic compartments (centre, red): DsRed-Rab11 (A); Ds-Rab5 (B); early endosomal antigen 1 (α-EEA1) (C); fluorescent transferrin (Alexa568-Tf was applied 10 min before fixation) (D); DsRed-Rab7 (E); lysosomal associated membrane protein 1 (α-LAMP-1) (F) and DsRed-Rab9 (G). After 8 h cells were fixed and stained with antibodies (where indicated) and analysed with a confocal microscope. Colocalization is depicted in yellow (right panel). Insets show a magnification of the regions marked with dotted lines. (H) Quantification of the area of colocalization of EGFP-SetA with the indicated marker proteins and of each marker protein with EGFP-SetA was determined by using areas of the cell enriched in both signals such as those shown in A-G. At least five independent cells and two distinct microscopic stack layers were measured for colocalization with the quantification software from Metamorph. Scale bar, 10 μm.

with various phosphoinositide lipids and also in binding studies performed with preparations of artificial vesicles that were enriched with the specific type of lipids. In addition, using surface plasmon resonance spectroscopy we determined the affinity of SetA for PtdIns(3)P. The K_d value of ~800 nM for the interaction of SetA with PtdIns(3)P is comparable with the K_d value of 430 nM obtained for the interaction of p40phox with PtdIns(3)P.

Phosphatidylinositol phosphates have been implicated in membrane trafficking through its interactions with specific proteins on endosomes. PtdIns(3)P is a major determinant of early endosomes, and the lipid appears to participate in many aspects of endosomal function, including, phagocytosis and turnover of cellular constituents (Gillooly *et al*., 2003; Burman and Ktistakis, 2010). In general, PtdIns(3)P is found on phagosomes (Ellson *et al*., 2001), and it was shown that PtdIns(3)P is essential for *Legionella* intracellular replication and participates in the modulation of the LCV, but seems not to be essential for phagocytosis (Weber *et al*., 2006). In contrast to PtdIns(3)P, PtdIns(4)P is produced at the ER or the Golgi and appears to be important for the regulation of secretory trafficking (Roth, 2004; Choudhury *et al*., 2005; Mayinger, 2009). Recently, it was shown that the *L. pneumophila* effector SidM/DrrA interacts specifically with PtdIns(4)P in order to be guided to its substrate Rab1 located at secretory vesicles (Brombacher *et al*., 2009; Schoebel *et al*., 2010). SidM/DrrA acts as a guanine nucleotide exchange factor and adenylyltransferase on Rab1 (Ingmundson *et al*., 2007; Machner and Isberg, 2007; Muller *et al*., 2010). Additionally, PtdIns(4)P was found to anchor the *Legionella* effector proteins SidC and SdcA to the *Legionella*-containing vacuole, but the precise function of these effectors is not yet known (Ragaz *et al*., 2008). Recently, it was found that the *L. pneumophila* virulence factor LpnE binds preferentially PtdIns(3)P and thereby associates with inositol polyphosphate 5-phosphatase OCRL1 on the replicative vacuole (Weber *et al*., 2009b). Here, we show that SetA harbours a PtdIns(3)P-binding domain in the C-terminus, which seems to be unique in amino acid sequence and not observed in other proteins in nature. Up to date there are only two PtdIns(3)P-domains known (FYVE-domain and p40phox PX-domain). It would be of general interest to obtain a structural view into the mechanism underlying the specific binding of SetA to PtdIns(3)P. Thus, the PtdIns(3)P-binding domain of SetA might be a valuable tool as marker for localization and analyses of the function of phosphoinositides in eukaryotic cells.

We observed that SetA associated with phagosomes, containing either *E. coli* or *L. pneumophila*, shortly after infection. And we also show that SetA binds to Rab5-containing endosomes (early endosomes) and not predominantly to Rab7-containing vesicles (late endosomes) or lysosomes as suggested previously (Heidtman *et al*., 2009). Therefore, we propose that after secretion into the host cytosol, SetA is attracted by LCV-containing PtdIns(3)P and, thereby, guided to its substrate for glucosylation which might be involved in the initial steps of LCV maturation.

Although it was reported that *L. pneumophila* lacking SetA exhibited no reduced replication in macrophages or *D. discoideum* (Heidtman *et al*., 2009), our data support recent findings that delivery of SetA into yeast causes strong growth defects (Heidtman *et al*., 2009). Moreover, we demonstrate a strong phenotype in mammalian cells after microinjection of SetA. The phenotype, shown in yeast, depends on both the C- and N-terminal domains of SetA, as only full-length protein or a combination of the separate domains were able to produce a strong growth defect. On the basis of these observations and recent findings from Isberg and co-workers (Heidtman *et al*., 2009), we suggest that SetA is a multidomain protein possessing a N-terminal glucosyltransferase domain and a C-terminal PtdIns(3)P-binding domain, which are both crucial for full activity.

Experimental procedures

Materials, bacterial and yeast strains, and plasmids

DNA-modifying enzymes were from Fermentas (St Leon-Rot, Germany). Phusion High-Fidelity DNA Polymerase was from New England Biolabs (Ipswich, MA, USA) and PfuII Turbo DNA Polymerase was from Stratagene (Waldbronn, Germany). UDP-[^{14}C]glucose and UDP-[^{14}C]N-acetyl-glucosamine was from Biotrend (Cologne, Germany). UDP-[^{14}C]galactose was from PerkinElmer Life Sciences (Rodgau, Germany). Histone type II preparation from calf thymus was from Sigma-Aldrich. Alexa568 labelled transferrin was from Invitrogen. pET28a vector were

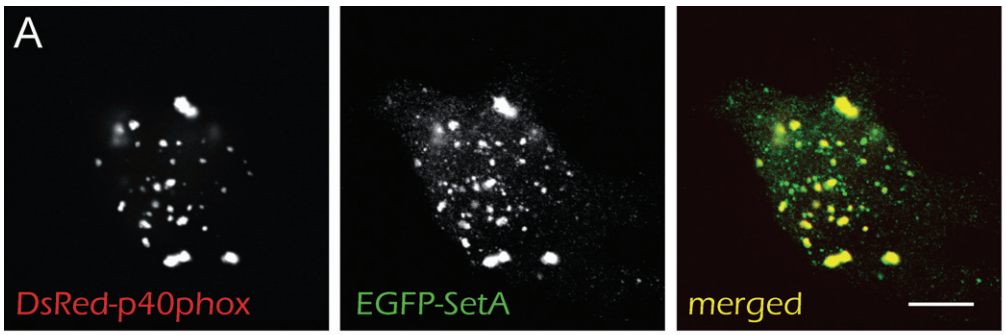
A
DsRed-p40phox
EGFP-SetA
merged

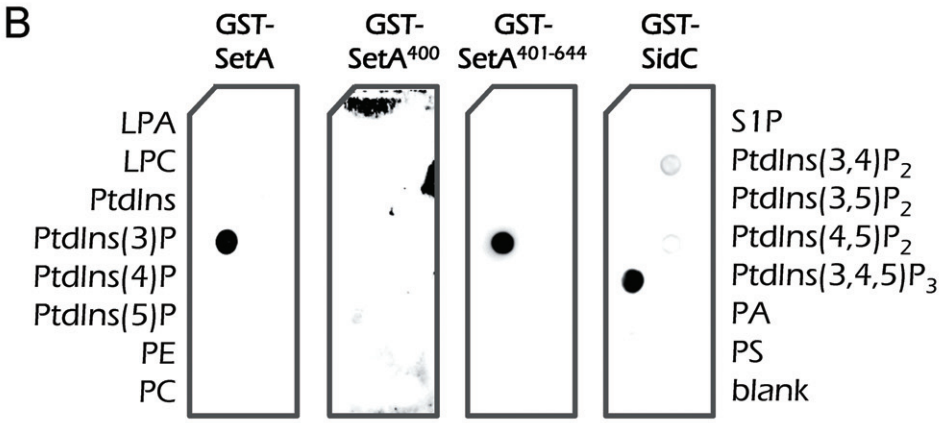
B
GST-SetA
GST-SetA400
GST-SetA401-644
GST-SidC
LPA
LPC
PtdIns
PtdIns(3)P
PtdIns(4)P
PtdIns(5)P
PE
PC
S1P
PtdIns(3,4)P2
PtdIns(3,5)P2
PtdIns(4,5)P2
PtdIns(3,4,5)P3
PA
PS
blank

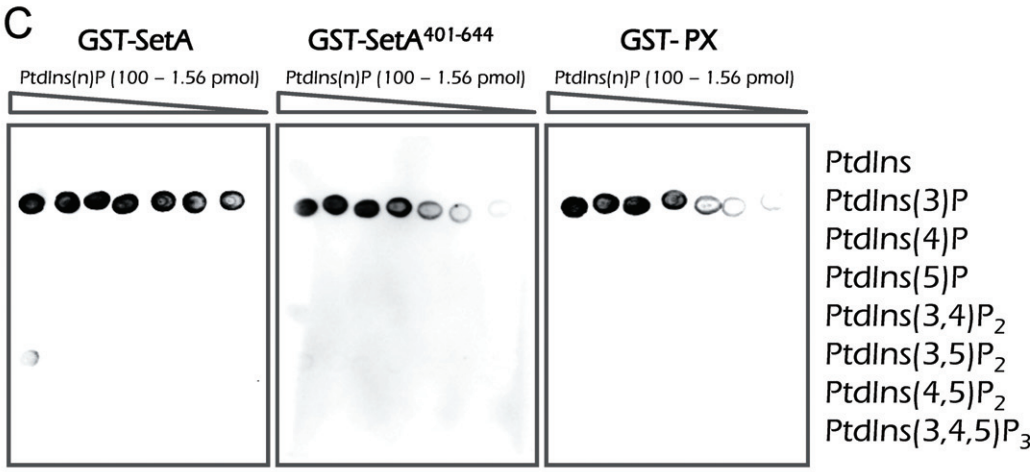
C
GST-SetA
GST-SetA401-644
GST- PX
PtdIns(n)P (100 – 1.56 pmol)
PtdIns(n)P (100 – 1.56 pmol)
PtdIns(n)P (100 – 1.56 pmol)
PtdIns
PtdIns(3)P
PtdIns(4)P
PtdIns(5)P
PtdIns(3,4)P2
PtdIns(3,5)P2
PtdIns(4,5)P2
PtdIns(3,4,5)P3

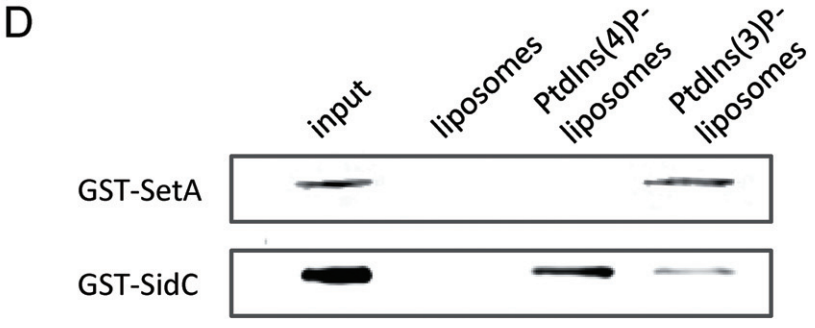
D
input
liposomes
PtdIns(4)P-liposomes
PtdIns(3)P-liposomes
GST-SetA
GST-SidC

Fig. 6. SetA specifically interacts with PtdIns(3)P.
A. Confocal micrographs of cotransfected HeLa cells with EGFP-SetA (green, centre) and the p40phox PX domain of NADPH oxidase (DsRed, left) colocalizing with PtdIns(3)P containing vesicles. Colocalization is shown in yellow (right). Scale bar, 10 μm.
B. Protein-phospholipid overlay assay with GST-SetA (12 nM), the catalytic domain GST-SetA^{400} (12 nM), the C-terminal domain GST-SetA$^{401–644}$ (12 nM) and GST-SidC (160 nM) as a control protein, which binds specifically to PtdIns(4)P. Nitrocellulose membranes pre-spotted with 100 pmol phospholipids were incubated with the indicated proteins and probed with an anti-GST antibody. Left lanes: lysophosphatidic acid (LPA), lysophosphocholine (LPC), phosphatidylinositol (PtdIns), phosphatidylinositol phosphate [PtdIns(n)P], phosphatidylethanolamine (PE), phosphatidylcholine (PC). Right lanes: sphingosine-1-phosphate (S1P), phosphatidylinositol phosphate (PtdIns(n)P), phosphatidic acid (PA), phosphatidylserine (PS).
C. Phosphatidylinositide array with GST-SetA, the C-terminal domain GST-SetA$^{401–644}$ and GST-p40phox PX-domain (PI3P-Grip) as PtdIns(3)P-binding control. Nitrocellulose membranes pre-spotted with twofold serial dilution of the indicated phosphatidylinositides [PtdIns(n)P] (100 to 1.56 pmol) were overlayed with 12 nM of each GST fusion protein. After extensive washing, proteins were detected with an anti-GST antibody.
D. SetA association with PtdIns(3)P-containing liposomes. Liposomes consisting of phosphatidylcholine and PtdIns(3)P or PtdIns(4)P (each 1%), respectively, were incubated with GST-SetA and GST-SidC (each 500 nmol) as PtdIns(4)P binding control. Liposomes without phosphoinositides were used as negative control. After centrifugation and washing, liposomes were Western-blotted and probed with an anti-GST antibody.

from Novagen (Madison, WI, USA), expression vectors pGEX-4T1 and pGEX-4T3 were from GE Healthcare. *E. coli* TG1 was used for general cloning and protein expression of pGEX constructs. *E. coli* BL21 (DE3) CodonPlus (Stratagene) were used for protein expression of pET constructs. Yeast vectors pESC-Ura and pESC-His were from Agilent Technologies (Waldbronn, Germany). *Saccharomyces cerevisiae* MH272-3fα (ura3 leu2 his3 trp1 ade2) was a kind gift from Sabine Rospert (Institute for Biochemistry and Microbiology, University of Freiburg, Germany). The protein GST-SidC was kindly provided by Hubert Hilbi [Max von Pettenkofer-Institute, University of Munich (LMU), Germany]. Recombinant Rac1 and the glucosyltransferase domain of *C. difficile* toxin B were prepared as described earlier (Jank *et al.*, 2007). The following plasmids were from Addgene (http://www.addgene.org): pDSRed-Rab7 WT (Plasmid 12661), DsRed-Rab9 WT (Plasmid 12677), DsRed-rab11 WT (Plasmid 12679)

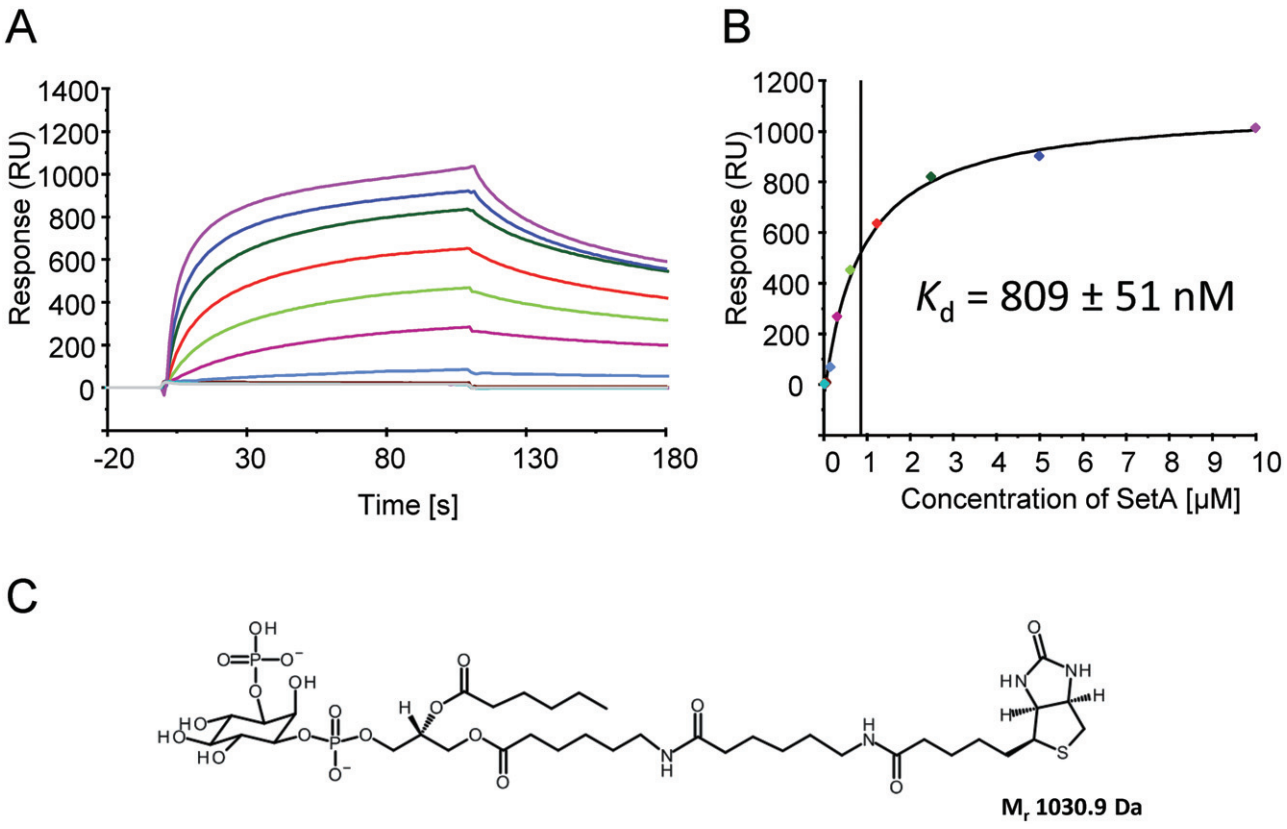

Fig. 7. High affinity interaction of SetA with PtdIns(3)P.
A. Surface plasmon resonance (SPR) spectroscopy of SetA binding to biotin-PtdIns(3)P immobilized to a streptavidin-coated sensor chip. A representative sensogram shows the binding of SetA to the surface bound PtdIns(3)P. SetA was diluted in a twofold consecutive dilution series ranging from 10 μM to 19.5 nM and flowed over the chip.
B. Equilibrium binding analysis indicates a K_d of 809 ± 51 nM (SD) ($n = 4$).
C. Chemical structure of the biotin-labelled PtdIns(3)P derivative used for SPR.

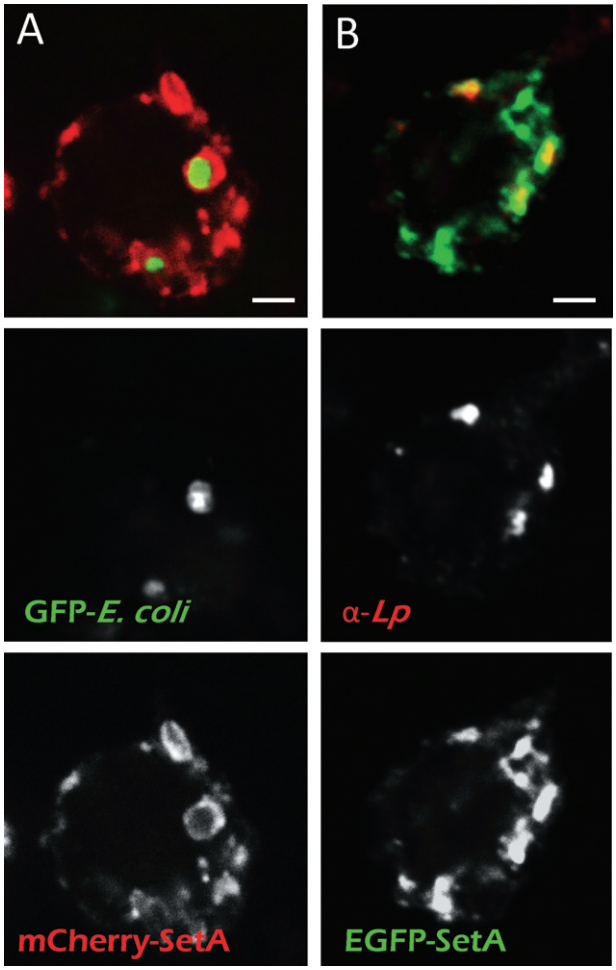

Fig. 8. SetA localizes to the phagosome.
A. RAW 264.7 macrophages were transfected with pmCherry SetA (red). After 8 h incubation at cell culture conditions, cells were infected with *E. coli* expressing GFP (moi = 50) and incubated for additional 2 h in order to be phagocytized. After extensive washing and PFA-fixation, cells were analysed by confocal microscopy.
B. RAW 264.7 macrophages expressing EGFP-SetA were infected with *L. pneumophila* serogroup 1 Phil. 1 (*Lp*) (moi = 100) for 1 h, washed with pre-warmed medium and incubated for additional 1 h. After fixation, cells were immunostained with anti-*Legionella* major outer membrane protein 1 (MOMP-1) and analysed with a confocal microscope. Scale bar, 10 μm. For quantification, at least 25 vacuoles containing bacteria from three independent experiments were taken and the amount of colocalization of bacteria and SetA determined (see text).

(Choudhury *et al.*, 2002), p40PX-EGFP (Plasmid 19010) (Kanai *et al.*, 2001). All other reagents were of analytical grade and purchased from commercial sources.

Cloning of genes for bacterial, yeast and mammalian expression

The genes SetA (lpg1978), were amplified with Phusion DNA-polymerase from the genomic DNA of *L. pneumophila* strain Philadelphia-1 and cloned into a modified pET28a vector with an introduced TEV protease cleavage site (Belyi *et al.*, 2008). Cloning of pEGFP-SetA, pmCherry SetA, pDsRed-SetA, pESC-Ura SetA, pESC-His SetA, pET28a TEV SetA, pGEX4T3 SetA and truncation mutants were performed with oligonucleotide primers with additional restriction sites for BamHI and SalI or HindIII (Table S1) with the corresponding vector digested with BamHI or BglII, and SalI or HindIII. The gene of the PX-domain aa 1–148 was excised from the plasmid p40PX-EGFP with BglII and HindIII and ligated into BglII/HindII cleaved pDsRed C1-vector; pDsRed-Rab5 was constructed in the same manner by using pEGFP-N3 Rab5. QuikChange Kit (Stratagene La Jolla, CA, USA) in combination with Pfu Turbo DNA polymerase was used for the replacement of one to three nucleotides using the oligonucleotides shown in Table S1. All sequences of corresponding plasmids were confirmed by sequencing (GATC, Konstanz, Germany).

Recombinant protein expression

Escherichia coli BL21(DE3) codon plus were transformed with the desired plasmid and grown in the LB broth supplemented with chloramphenicol, in combination with ampicillin or kanamycin, depending on the plasmid used, on a shaker at 37°C until $A_{600} = 0.8$. Protein expression from the pET28-based plasmids was induced by 1 mM isopropyl-β-D-thiogalactopyranoside (Roth, Karlsruhe, Germany) for 4–5 h at 22°C, and for pGEX-based constructs with 0.2 mM isopropyl-β-D-thiogalactopyranoside at 37°C for 3 h. Bacterial cells were harvested by centrifugation at 6000 *g* for 15 min, resuspended in lysis buffer [50 mM Tris-HCl (pH 7.4), 150 mM NaCl, 25 mM imidazole, 30 μg ml^{-1} DNase I, 1 mM β-mercaptoethanol, and Proteinase Inhibitor Cocktail (Roche)] and lysed by French press. The cleared lysate was subjected to chromatography on a glutathione-Sepharose or nickel-equilibrated chelating Sepharose Fast Flow column according to the manufacturer's instructions (GE Healthcare). Bound proteins were eluted with 10 mM reduced glutathione, 0.5 M imidazole or thrombin treatment, depending on the construct used.

Cell culture, transient transfection

HeLa cells were cultured in Dulbecco's modified Eagle's medium (DMEM) supplemented with 10% fetal calf serum (FCS), 1% nonessential amino acids and 1% sodium pyruvate (Biochrom, Berlin, Germany). For immunostainings, cells were plated on HCl-washed coverslips. For live cell imaging, cells were plated on glass bottom dishes (Mattek, Ashland, MA, USA). HeLa cells were transfected using Lipofectamine 2000 (Invitrogen) according to the manufacturers' instructions. Raw 264.7 macrophages were cultured in DMEM supplemented with 10% fetal calf serum (FCS). Raw 264.7 cells were transfected using polyethyleneimine as reported earlier (Ehrhardt *et al.*, 2006). Briefly, 1 μg DNA and 2.5 μl PEI [polyethyleneimine (1 mg ml^{-1})] were combined in 50 μl DMEM medium and incubated at room temperature for 15 min. The mixture was applied to cells, which starved for 1 h in DMEM medium without additives, and incubated for additional 2 h before medium was exchanged to full medium and incubated for indicated times.

Microinjection studies

For microinjection, embryonic bovine lung (EBL) cells were seeded on HCl-washed glass coverslips at about 10^4 cells per

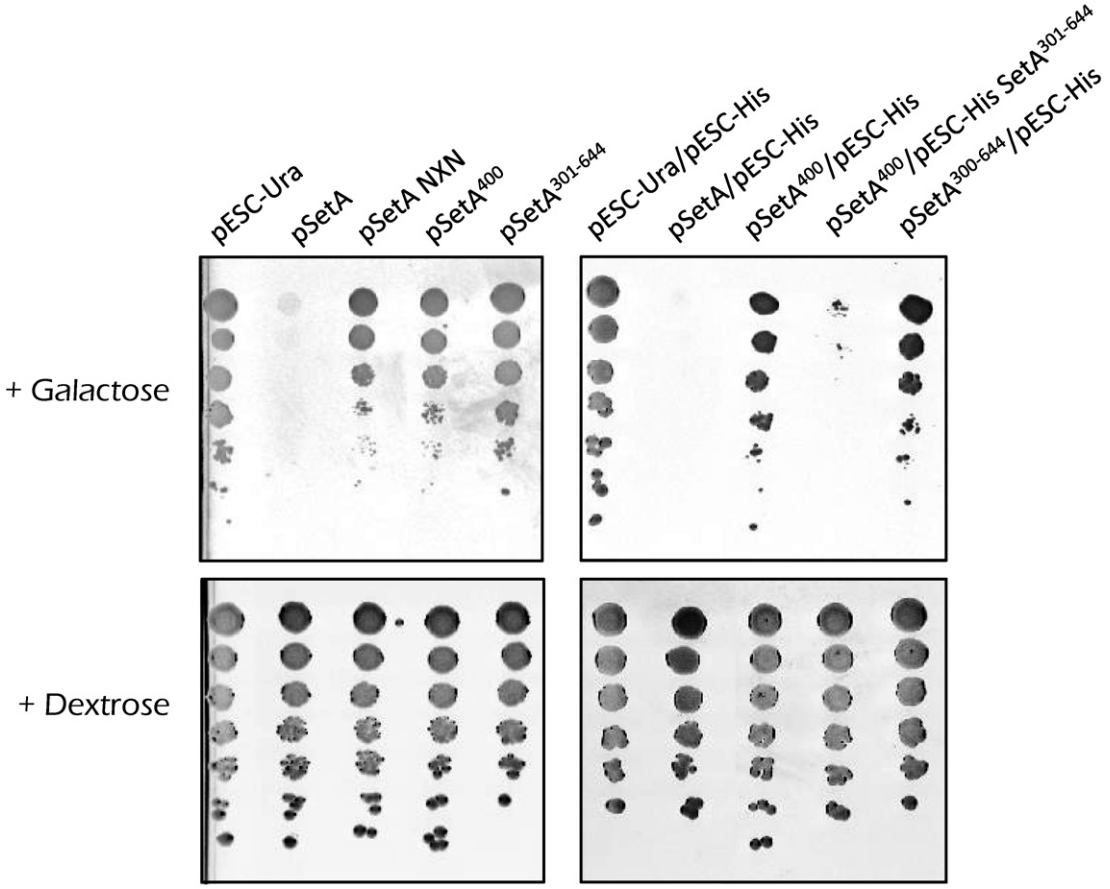

Fig. 9. The N- and C-terminus of SetA are required for cellular effects. Growth of yeast cells expressing SetA, SetA NXN or SetA truncations (indicated) from a galactose-inducible promoter on galactose medium (upper panels) or on dextrose medium as input control (lower panels). Yeast strains harbouring empty vectors (pESC-Ura, pESC-His or both) were used as control. Fivefold serially diluted yeast cultures grown in glucose medium were spotted followed by incubation at 37°C for 4 days.

30 mm dish and cultivated for 24 h in DMEM supplemented with 10% fetal calf serum in humidified 5% CO_2 at 37°C. Microinjection was performed with Femtotips II and the microinjector 5242 and micromanipulator 5171 from Eppendorf. Alexa488 and Alexa562 coupled secondary antibodies (Invitrogen) were used as markers for microinjection.

Live cell imaging

For live cell imaging, cells were incubated in a homebuilt microincubator that provided a humidified atmosphere (6.5% CO_2 and 9% O_2) at 37°C on a Zeiss Axiovert 200 M inverted microscope (Carl Zeiss, Jena, Germany). Differential interference contrast images were collected with a digital camera (Coolsnap HQ, Roper Scientific, Tucson, AZ, USA) driven by Metamorph imaging software (Universal Imaging, Downingtown, PA, USA). For the observation of morphological alterations of EBL-cells or HeLa-cells, time-lapse series were acquired with the indicated time intervals.

Antibodies and fluorescent dyes

Rabbit anti-Rab5 (sc-598), mouse anti-LAMP1 (sc-20011), and mouse anti-LAMP2 (sc-20004) were from Santa Cruz Biotechnology (CA, USA), rabbit anti-EEA1 (ab50313) and mouse anti-Rab7 (ab50533) were from abcam (Cambridge, UK). Alexa568 labelled transferrin and all secondary Alexa568- and Alexa488-conjugated antibodies were purchased from Invitrogen.

Immunostaining

Cells were washed with phosphate-buffered saline (PBS) at room temperature, fixed with 4% formaldehyde in PBS, washed again, and permeabilized with 0.15% Triton X-100 in PBS. Cells were blocked by 1% BSA and 0.05% Tween 20 in PBS for 30 min. Incubation with primary antibody (anti-LAMP1, anti-LAMP2, anti-Rab5, anti-Rab7) was overnight at 4°C in 1:200 dilutions with blocking solution. The samples were then washed with 0.05% Tween 20 in PBS and incubated with 1:200 dilutions of the secondary antibodies in blocking solution for 1.5 h at room temperature. Thereafter, cells were washed again and embedded with Mowiol supplemented with 1,4-diazobicyclo[2.2.2]octane (Sigma). Fixed samples were analysed with an inverted Axiovert 200 M microscope (Carl Zeiss) equipped with plan-apochromat objectives, with a monochromator (Cairn Optoscan, Faversham Kent, UK) and suitable filters. Images were collected with a digital camera (Coolsnap HQ, Roper Scientific) driven by Metamorph imaging software (Universal Imaging). Confocal images were

collected with a Yokogawa CSU-X1 spinning disc confocal head (Tokyo, Japan) with an emission filter wheel, a Coolsnap HQ II digital camera, with 488 nm and 561 nm laser lines.

Protein lipid overlay (PLO) assay

PLO assay was performed with lipid strips and PIP-arrays from Echelon Biosciences (Salt Lake City, USA) as described earlier (Dowler *et al.*, 2002).

Nitrocellulose membranes pre-spotted with different phospholipids were blocked with 3% fat-free BSA in TBST [50 mM Tris, 150 mM NaCl and 0.1% Tween-20 (v/v) pH 7.5] for 1 h at room temperature and incubated with GST-fusion proteins (12 nM in 2 ml blocking buffer) overnight at 4°C. Binding of the GST-fusion proteins to lipids was visualized with an anti-GST antibody (GE Healthcare) and a secondary peroxidase-coupled anti-goat antibody (Santa Cruz Biotechnology).

PtdInsP-liposome binding assay

To test whether SetA binds to phosphoinositides incorporated into phospholipid vesicles, we prepared liposomes consisting of solely 1 mM phosphatidylcholine (liposomes) and liposomes containing 1% PtdIns(3)P (Echelon Biosciences) or 1% PtdIns(4)P (Echelon Biosciences) with an average size of 11 $\pm$ 5 μm by extruding 5 times through a 26G needle. The vesicles were incubated with GST-fusion proteins (500 nM) in Hepes (10 mM, pH 7.5) in a final volume of 200 μl for 30 min at 4°C. Subsequently, liposomes were centrifuged for 30 min at 100 000 *g* and washed three times with 1 ml Hepes (10 mM pH 7.5). Finally, the pellet was resuspended in 20 μl of loading buffer, boiled and subjected to 12.5% SDS-PAGE. GST fusion proteins were visualized by Western blot with a monoclonal anti-GST antibody (GE Healthcare).

Hydrolysis of UDP-sugars by SetA

UDP-sugar hydrolysis was measured as described earlier for the glucosyltransferase toxin B from *Clostridium difficile* (Jank *et al.*, 2007). SetA fragments and mutants were incubated with 10 μM UDP-[^{14}C]-sugar in a buffer containing 50 mM Hepes (pH 7.5), 100 mM KCl, 2 mM $MgCl_2$ and 1 mM $MnCl_2$. Total volume was 10 μl. Samples of 800 nl were taken at each time point and subjected to PEI (polyethyleneimine)-cellulose thin layer chromatography (Merck, Darmstadt, Germany) with 0.2 mM LiCl as mobile phase to separate the hydrolysed sugar from intact UDP-sugar. The plates were dried and analysed by PhosphorImager analysis. Quantification was carried out with ImageQuant (Molecular Dynamics/GE Healthcare, Freiburg, Germany).

Glucosylation reaction

Recombinant SetA constructs (1 μM) or the glucosyltransferase domain of *C. difficile* toxin B (aa 1–543; 100 nM) were incubated with 50 μM UDP-[^{14}C]glucose in a buffer, containing 50 mM Hepes pH 7.4, 2 mM $MgCl_2$ and 1 mM $MnCl_2$ for 60 min at 30°C in the presence or absence of 10 μg histone preparation from calf thymus (Sigma) or recombinant Rac1 (1 μg). Total volume was 20 μl. Labelled proteins were analysed by SDS-PAGE followed by phosphorimaging (Molecular Dynamics/GE Healthcare, Freiburg, Germany).

Surface plasmon resonance spectroscopy

Interaction analysis was conducted at 25°C using a Biacore X100 biosensor (GE Healthcare) equipped with a SA sensor chip (GE Healthcare). Biotin-PtdIns(3)P (200 nM, Echelon Biosciences, Salt Lake City, USA) was diluted in HBS-EP+ running buffer (Hepes 10 mM, pH 7.4, 150 mM NaCl, EDTA 3 mM and 0.05% Tween 20) and injected across individual flow cells at a flow rate of 10 μl min^{-1} until response units (RU) reached 106.9. Fresh Ligand surfaces were post-conditioned by injecting three 60 s pulses of 1.0 M NaCl and 25 mM NaOH. Unmodified streptavidin flow cells served as reference and control surfaces. Analytes were buffer exchanged by gel filtration and diluted in HBS-EP+ running buffer in a serial 1:1 dilution, ranging from 10 μM to 19.5 nM, and applied for 60–110 s with a flow rate of 10 μl min^{-1} with subsequent washing steps of 500 s. A single pulse of guanidinium chloride (2 M) for 60 s was used to regenerate the sensor surfaces. Binding responses were referenced by subtracting the response generated across an unmodified streptavidin flow cell, and double referenced by subtracting an average buffer response (from at least two blank injections). Binding affinities were calculated using the Biacore X100 evaluation software.

Acknowledgements

We thank Peter Gebhardt for excellent technical assistance and Dina Tartakovskaya for valuable support in yeast molecular biology. We are grateful to Hubert Hilbi for providing GST-SidC. We thank Andreas Schlosser for MS/MS analyses. We are grateful to L. Didenko and N. Shevlyagina for scanning electron images. The study was financially supported by BIOSS and the Deutsche Forschungsgemeinschaft (Ak6/17-2).

References

Aktories, K., and Barbieri, J.T. (2005) Bacterial cytotoxins: targeting eukaryotic switches. *Nat Rev Microbiol* **3:** 397–410.

Belyi, Y., Niggeweg, R., Opitz, B., Vogelsgesang, M., Hippenstiel, S., Wilm, M., and Aktories, K. (2006) *Legionella pneumophila* glucosyltransferase inhibits host elongation factor 1A. *Proc Natl Acad Sci USA* **103:** 16953–16958.

Belyi, Y., Tabakova, I., Stahl, M., and Aktories, K. (2008) Lgt: a family of cytotoxic glucosyltransferases produced by *Legionella pneumophila*. *J Bacteriol* **190:** 3026–3035.

Belyi, Y., Jank, T., and Aktories, K. (2011) Effector glycosyltransferases in legionella. *Front Microbiol* **2:** 76.

Bravo, J., Karathanassis, D., Pacold, C.M., Pacold, M.E., Ellson, C.D., Anderson, K.E., *et al.* (2001) The crystal structure of the PX domain from p40(phox) bound to phosphatidylinositol 3-phosphate. *Mol Cell* **8:** 829–839.

Brombacher, E., Urwyler, S., Ragaz, C., Weber, S.S., Kami, K., Overduin, M., and Hilbi, H. (2009) Rab1 guanine nucleotide exchange factor SidM is a major phosphatidylinositol 4-phosphate-binding effector protein of *Legionella pneumophila*. *J Biol Chem* **284:** 4846–4856.

Burman, C., and Ktistakis, N.T. (2010) Regulation of autophagy by phosphatidylinositol 3-phosphate. *FEBS Lett* **584:** 1302–1312.

Busch, C., Hofmann, F., Selzer, J., Munro, J., Jeckel, D., and Aktories, K. (1998) A common motif of eukaryotic glycosyltransferases is essential for the enzyme activity of large clostridial cytotoxins. *J Biol Chem* **273:** 19566–19572.

Cho, W., and Stahelin, R.V. (2005) Membrane-protein interactions in cell signaling and membrane trafficking. *Annu Rev Biophys Biomol Struct* **34:** 119–151.

Choudhury, A., Dominguez, M., Puri, V., Sharma, D.K., Narita, K., Wheatley, C.L., *et al*. (2002) Rab proteins mediate Golgi transport of caveola-internalized glycosphingolipids and correct lipid trafficking in Niemann-Pick C cells. *J Clin Invest* **109:** 1541–1550.

Choudhury, R.R., Hyvola, N., and Lowe, M. (2005) Phosphoinositides and membrane traffic at the trans-Golgi network. *Biochem Soc Symp* **72:** 31–38.

De Camilli, P., Emr, S.D., McPherson, P.S., and Novick, P. (1996) Phosphoinositides as regulators in membrane traffic. *Science* **271:** 1533–1539.

Di Paolo, G., and De Camilli, P. (2006) Phosphoinositides in cell regulation and membrane dynamics. *Nature* **443:** 651–657.

Dowler, S., Kular, G., and Alessi, D.R. (2002) Protein lipid overlay assay. *Sci STKE* **2002:** l6.

Ehrhardt, C., Schmolke, M., Matzke, A., Knoblauch, A., Will, C., Wixler, V., and Ludwig, S. (2006) Polyethylenimine, a cost-effective transfection reagent. *Signal Transduct* **6:** 179–184.

Ellson, C.D., Anderson, K.E., Morgan, G., Chilvers, E.R., Lipp, P., Stephens, L.R., and Hawkins, P.T. (2001) Phosphatidylinositol 3-phosphate is generated in phagosomal membranes. *Curr Biol* **11:** 1631–1635.

Ensminger, A.W., and Isberg, R.R. (2009) *Legionella pneumophila* Dot/Icm translocated substrates: a sum of parts. *Curr Opin Microbiol* **12:** 67–73.

de Felipe, K.S., Pampou, S., Jovanovic, O.S., Pericone, C.D., Ye, S.F., Kalachikov, S., and Shuman, H.A. (2005) Evidence for acquisition of *Legionella* type IV secretion substrates via interdomain horizontal gene transfer. *J Bacteriol* **187:** 7716–7726.

Gillooly, D.J., Raiborg, C., and Stenmark, H. (2003) Phosphatidylinositol 3-phosphate is found in microdomains of early endosomes. *Histochem Cell Biol* **120:** 445–453.

Heidtman, M., Chen, E.J., Moy, M.Y., and Isberg, R.R. (2009) Large-scale identification of *Legionella pneumophila* Dot/Icm substrates that modulate host cell vesicle trafficking pathways. *Cell Microbiol* **11:** 230–248.

Hubber, A., and Roy, C.R. (2010) Modulation of host cell function by *Legionella pneumophila* type IV effectors. *Annu Rev Cell Dev Biol* **26:** 261–283.

Hurley, J.H. (2006) Membrane binding domains. *Biochim Biophys Acta* **1761:** 805–811.

Ingmundson, A., Delprato, A., Lambright, D.G., and Roy, C.R. (2007) *Legionella pneumophila* proteins that regulate Rab1 membrane cycling. *Nature* **450:** 365–369.

Isberg, R.R., O'Connor, T.J., and Heidtman, M. (2009) The *Legionella pneumophila* replication vacuole: making a cosy niche inside host cells. *Nat Rev Microbiol* **7:** 13–24.

Jank, T., Giesemann, T., and Aktories, K. (2007) Clostridium difficile glucosyltransferase toxin B – essential amino acids for substrate-binding. *J Biol Chem* **282:** 35222–35231.

Just, I., Selzer, J., Wilm, M., Von Eichel-Streiber, C., Mann, M., and Aktories, K. (1995a) Glucosylation of Rho proteins by *Clostridium difficile* toxin B. *Nature* **375:** 500–503.

Just, I., Wilm, M., Selzer, J., Rex, G., Von Eichel-Streiber, C., Mann, M., and Aktories, K. (1995b) The enterotoxin from *Clostridium difficile* (ToxA) monoglucosylates the Rho proteins. *J Biol Chem* **270:** 13932–13936.

Kanai, F., Liu, H., Field, S.J., Akbary, H., Matsuo, T., Brown, G.E., *et al*. (2001) The PX domains of p47phox and p40phox bind to lipid products of PI(3)K. *Nat Cell Biol* **3:** 675–678.

Lemmon, M.A. (2008) Membrane recognition by phospholipid-binding domains. *Nat Rev Mol Cell Biol* **9:** 99–111.

Machner, M.P., and Isberg, R.R. (2006) Targeting of host Rab GTPase function by the intravacuolar pathogen *Legionella pneumophila*. *Dev Cell* **11:** 47–56.

Machner, M.P., and Isberg, R.R. (2007) A bifunctional bacterial protein links GDI displacement to Rab1 activation. *Science* **318:** 974–977.

Mayinger, P. (2009) Regulation of Golgi function via phosphoinositide lipids. *Semin Cell Dev Biol* **20:** 793–800.

Mayle, K.M., Le, A.M., and Kamei, D.T. (2011) The intracellular trafficking pathway of transferrin. *Biochim Biophys Acta* (in press).

Mukherjee, S., Liu, X., Arasaki, K., McDonough, J., Galan, J.E., and Roy, C.R. (2011) Modulation of Rab GTPase function by a protein phosphocholine transferase. *Nature* **477:** 103–106.

Muller, M.P., Peters, H., Blumer, J., Blankenfeldt, W., Goody, R.S., and Itzen, A. (2010) The *Legionella* effector protein DrrA AMPylates the membrane traffic regulator Rab1b. *Science* **329:** 946–949.

Murata, T., Delprato, A., Ingmundson, A., Toomre, D.K., Lambright, D.G., and Roy, C.R. (2006) The *Legionella pneumophila* effector protein DrrA is a Rab1 guanine nucleotide-exchange factor. *Nat Cell Biol* **8:** 971–977.

Nagai, H., Kagan, J.C., Zhu, X., Kahn, R.A., and Roy, C.R. (2002) A bacterial guanine nucleotide exchange factor activates ARF on *Legionella* phagosomes. *Science* **295:** 679–682.

Neunuebel, M.R., Chen, Y., Gaspar, A.H., Backlund, P.S., Jr, Yergey, A., and Machner, M.P. (2011) De-AMPylation of the small GTPase Rab1 by the pathogen *Legionella pneumophila*. *Science* **333:** 453–456.

Ninio, S., and Roy, C.R. (2007) Effector proteins translocated by *Legionella pneumophila*: strength in numbers. *Trends Microbiol* **15:** 372–380.

Ragaz, C., Pietsch, H., Urwyler, S., Tiaden, A., Weber, S.S., and Hilbi, H. (2008) The *Legionella pneumophila* phosphatidylinositol-4 phosphate-binding type IV substrate SidC recruits endoplasmic reticulum vesicles to a replication-permissive vacuole. *Cell Microbiol* **10:** 2416–2433.

Reinert, D.J., Jank, T., Aktories, K., and Schulz, G.E. (2005) Structural basis for the function of *Clostridium difficile* Toxin B. *J Mol Biol* **351:** 973–981.

Roth, M.G. (2004) Phosphoinositides in constitutive membrane traffic. *Physiol Rev* **84:** 699–730.

Sato, T.K., Overduin, M., and Emr, S.D. (2001) Location, location, location: membrane targeting directed by PX domains. *Science* **294:** 1881–1885.

Schoebel, S., Blankenfeldt, W., Goody, R.S., and Itzen, A. (2010) High-affinity binding of phosphatidylinositol 4-phosphate by *Legionella pneumophila* DrrA. *EMBO Rep* **11:** 598–604.

Schoebel, S., Cichy, A.L., Goody, R.S., and Itzen, A. (2011) Protein LidA from *Legionella* is a Rab GTPase supereffector. *Proc Natl Acad Sci USA* **108:** 17945–17950.

Shohdy, N., Efe, J.A., Emr, S.D., and Shuman, H.A. (2005) Pathogen effector protein screening in yeast identifies *Legionella* factors that interfere with membrane trafficking. *Proc Natl Acad Sci USA* **102:** 4866–4871.

Tan, Y., and Luo, Z.Q. (2011) *Legionella pneumophila* SidD is a deAMPylase that modifies Rab1. *Nature* **475:** 506–509.

Tan, Y., Arnold, R.J., and Luo, Z.Q. (2011) *Legionella pneumophila* regulates the small GTPase Rab1 activity by reversible phosphorylcholination. *Proc Natl Acad Sci USA* **108:** 21212–21217.

Weber, S.S., Ragaz, C., Reus, K., Nyfeler, Y., and Hilbi, H. (2006) *Legionella pneumophila* exploits PI(4)P to anchor secreted effector proteins to the replicative vacuole. *PLoS Pathog* **2:** e46.

Weber, S.S., Ragaz, C., and Hilbi, H. (2009a) Pathogen trafficking pathways and host phosphoinositide metabolism. *Mol Microbiol* **71:** 1341–1352.

Weber, S.S., Ragaz, C., and Hilbi, H. (2009b) The inositol polyphosphate 5-phosphatase OCRL1 restricts intracellular growth of *Legionella*, localizes to the replicative vacuole and binds to the bacterial effector LpnE. *Cell Microbiol* **11:** 442–460.

Supporting information

Additional Supporting Information may be found in the online version of this article:

Fig. S1. Surface plasmon resonance (SPR) spectroscopy of SetA NXN, SetA$^{301–644}$, GST-p40phox and GST. Representative SPR-sensograms (left panel) of the indicated proteins binding to biotin-PtdIns(3)P immobilized on a streptavidin-coated sensor chip. Proteins were diluted in consecutive dilution series from 10 μM to 19.5 nM and flowed over the chip. Right panel: Resonance signal units were fitted against the concentration of the indicated proteins for determination of the dissociation constants.
A. SPR-sensogram of the catalytic inactive DXD-mutant, SetA NXN. Equilibrium binding analysis of SetA NXN indicates a K_d value of 1.01 ± 0.22 μM.
B. The SPR-sensogram of SetA$^{301–644}$ shows similar results with a K_d value of 1.45 ± 0.28 μM.
C and D. The GST-p40phox PX domain of the NADPH oxidase was used as a positive control with a binding constant of K_d = 431 ± 27 nM (C) and GST alone as negative control (D). All experiments were performed as triplicates.

Table S1. List of oligonucleotide primers.

Movie S1. Life cell imaging of embryonic bovine lung (EBL) cells microinjected with recombinant SetA (5 μg μl^{-1}). Cells were photographed each minute for 8 h. Microinjected cells were distinguished by using an Alexa488 labelled antibody (see immunofluorescent image in Fig. 1C, first panel). Cinepak Codec by Radius was used for compression. Scale bar, 20 μm.

Movie S2. Life cell imaging of embryonic bovine lung (EBL) cells microinjected with recombinant SetA NXN (5 μg μl^{-1}), the catalytic inactive DXD mutant. Cells were photographed each minute for 8 h. Microinjected cells were distinguished by using an Alexa568 labelled antibody (see immunofluorescent image in Fig. 1D, first panel). Cinepak Codec by Radius was used for compression. Scale bar, 20 μm.

Movie S3. Localization of SetA with motile vesicles. Live cell imaging of HeLa cells expressing EGFP-SetA. Micrographs were taken 8 h after pEGFP-SetA transfection in 5 s intervals for 3 min. Cinepak Codec by Radius was used for compression. Scale bar, 10 μm.

Movie S4. Localization of SetA with Rab5-containing vesicles. Cotransfection of HeLa cells with DsRed-Rab5 (red) and EGFP-SetA (green). Micrographs were taken 8 h after transfection in 4 s intervals for 4 min. Cinepak Codec by Radius was used for compression.